energies

MDPI

Article

Investigation of Adaptive Droop Control Applied to Low-Voltage DC Microgrid

Prudhvi Kumar Gorijeevaram Reddy *, Sattianadan Dasarathan * and Vijayakumar Krishnasamy *

Department of Electrical and Electronics Engineering, SRM Institute of Science and Technology, Chennai 603203, India

* Correspondence: eeecd.pruddu@gmail.com (P.K.G.R.); sattiand@srmist.edu.in (S.D.); kvijay_srm@rediffmail.com (V.K.)

Abstract: In a DC microgrid, droop control is the most common and widely used strategy for managing the power flow from sources to loads. Conventional droop control has some limitations such as poor voltage regulation and improper load sharing between converters during unequal source voltages, different cable resistances, and load variations. This paper addressed the limitations of conventional droop control by proposing a simple adaptive droop control technique. The proposed adaptive droop control method was designed based on mathematical calculations, adjusting the droop parameters accordingly. The primary objective of the proposed adaptive droop controller was to improve the performance of the low-voltage DC microgrid by maintaining proper load sharing, reduced circulating current, and better voltage regulation. The effectiveness of the proposed methodology was verified by conducting simulation and experimental studies.

Keywords: DC microgrid; droop control; parallel operation; dc-dc converter; load sharing

Citation: Gorijeevaram Reddy, P.K.; Dasarathan, S.; Krishnasamy, V. Investigation of Adaptive Droop Control Applied to Low-Voltage DC Microgrid. *Energies* **2021**, *14*, 5356. https://doi.org/10.3390/en14175356

Academic Editor: Rasoul Shalchi Alishah

Received: 17 July 2021
Accepted: 24 August 2021
Published: 28 August 2021

1. Introduction

Recently, many researchers have been attracted to the development in integrating different power resources in a distributed approach. The proper integration between distributed energy resources, battery storage systems, and different loads connected through power electronic devices delivers quality of power to the consumers [1]. It is not necessary for the energy resources to be located at the same site; they can be located at different sites based on the ease of energy availability. There are a lot of advantages with distributed energy resources such as reliability, stability, expandability, power quality, and efficiency [2].

Based on the source of supply voltage, microgrids are categorized as AC and DC microgrids, with their main advantage being the capability of operating in islanded mode, as well as grid-connected mode [3,4]. Recently, extensive research works have been carried out on DC microgrids as they have more advantages over AC microgrids [5–9]. AC microgrids have to deal with the reactive power, skin effect, and many other power quality problems that are absent in DC microgrids. An architectural overview of an LVDC microgrid is presented in Figure 1. The rapid development and different nature of the load have established a wide range of DC microgrids [10–13]. This technical advancement leads to a reduction in the capital cost of distributed generation (DG). The operation of different types of DG to meet the load needs a parallel operation but causes improper load sharing between converters and circulating current due to the abrupt variations in the source, sudden changes in load, and parametric differences due to various constraints [14]. Studies in the literature have discussed the most popular techniques of load sharing such as active current sharing [15–17] and droop control [18–32]. The most familiar one is the master/slave technique, where, in the master/slave current method, a common bus is employed between DC converters for proper current sharing [15] and the generation of the required base voltage. Normally, in droop control, two parameters are taken into account.

The first one is voltage control, which ensures good voltage regulation, and the second one is current control, which enables equal current sharing between the converters. Two control loops using PI have been implemented to estimate the current values of voltage and line impedance that makes the controller robust.

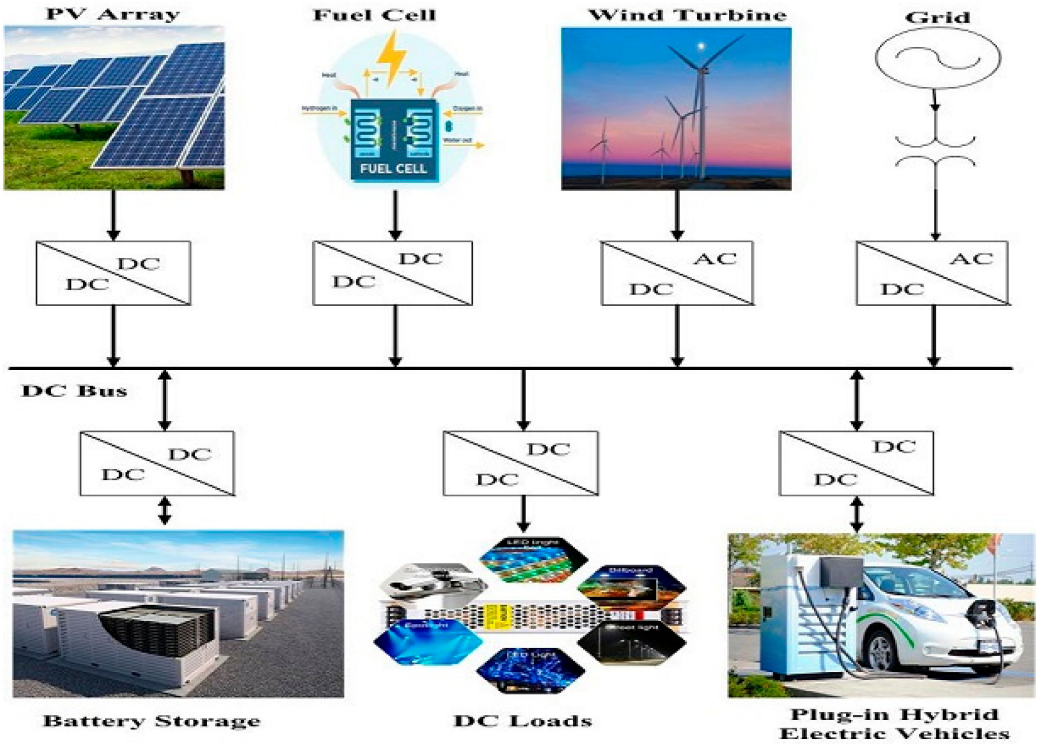

Figure 1. Architectural overview of LVDC microgrid.

One of the best distributed voltage controls is the droop control method, where the objective is to control the output voltage reference of each converter based on the output current of each converter [18]. The major limitations are improper load sharing between converters, poor voltage regulation, and a drop in voltage due to droop action. The role and prominence of cable resistance in load current distribution were discussed in [19]. The droop current sharing method without the requirement of any communication link was discussed in [20], and this method achieves smooth sharing of the load current among parallel modules using the droop of the load-regulation line of parallel-powered sources. A different droop method for the parallel operation of converters was proposed, which utilizes the base voltage of every unit to adjust and control automatically [21]. For the betterment of voltage regulation, a modified droop control was proposed [22], considering a virtual droop resistance as a function of the output voltage. Some of the major issues were not considered in the paper, mainly the impact of cable resistance. The parallel operation of buck converters with a voltage restoration control loop along with droop control was proposed [23]. The controller processes the demand and actual voltage values and generates the required restoration voltage. A modified lag compensator was developed and an alternative droop control method was proposed in [24], where different droop control methods such as V-I, I-V, and alternate I-V droop control were explained. The main limitation of the proposed method is the consideration of constant droop resistance. In [25], the circulating current issue that occurs with the variation in the converter output voltage was revealed. Droop index was introduced, which is a function considering normalized current sharing differences and the losses in the output side of converters. Although this method results in accurate load sharing, it involves considerable computational effort. In [26], the instantaneous virtual droop resistance reduced the circulating current and decreased the difference in the current sharing of converters. An advanced droop control method was proposed using an algorithm that improves power

sharing and output voltage stability by changing the resistance in the classical droop equation. A new strategy for current control to minimize the circulating current with a combination of average voltage and the proportional current sharing controller was proposed, considering fixed droop resistance [27]. In [28], an adaptive droop control method was proposed to suppress circulating currents in a low-voltage DC microgrid. Line resistances were estimated through mathematical calculation and droop parameters were adjusted accordingly. This method was accurate in load sharing and reducing the effect of line resistance, but the effect of the variation in source voltage or input parameters was not elevated. In [29], the proposed improved-mode adaptive droop control strategy for the DC microgrid considered various operating conditions and disturbance scenarios using the DC microgrid study system. The impact of distributed control methods was discussed in [30–32]. The importance and advantages of optimization techniques such as the stochastic optimization, consensus algorithm, and improved equal incremental principle (IEIP) in the distributed control methods were discussed in detail.

Many other research works have been carried out in a wide range to regulate the voltage on the DC bus and maintain proper current sharing with the consideration of load variation and cable resistance, but only little consideration has been given to the input variables such as input voltage and input current from the source side. In this paper, an algorithm was developed to ensure the robustness of control with the consideration of both input and output parameter variations.

2. Parallel Operation of DC–DC Converters in LVDC Microgrid

An LVDC microgrid was studied by considering two sources connected in parallel with dc–dc converters, and the phenomena of load sharing and circulating current occurrence during the parallel operation were projected. Considering the converters supplied with two different source voltages V_{i1} and V_{i2} and source currents I_{i1} and I_{i2}, different cases projecting the phenomena are given in Table 1. In Figure 2a, the output voltages, output currents, and converter 1 and 2 cable resistances are denoted as V_1, V_2, I_1, I_2, R_1, and R_2, respectively. In the equivalent circuit of the parallel operation of dc–dc converters, a voltage source in series with a cable resistance was considered for each converter output side, and is shown in Figure 2b.

Table 1. Different cases projecting the phenomena.

Case	Source Voltages V_{i1} and V_{i2}	Output Voltages V_1 and V_2	Cable Resistances R_1 and R_2	Output Currents I_1 and I_2	Circulating Current Phenomena
1	Same	Same	Equal	Equal	Absent
2	Same	Same	Unequal	Unequal	Absent
3	Distinct	Distinct	Equal	Unequal	Present
4	Distinct	Distinct	Unequal	Unequal	Present

Figure 2b shows the parallel connection of the DC–DC buck converter and its equivalent circuit. Applying KVL to the circuit, the following equations are obtained.

$$V_1 - I_1R_1 - I_LR_L = 0 \quad (1)$$

$$V_2 - I_2R_2 - I_LR_L = 0 \quad (2)$$

By using Equations (1) and (2), the converter output currents I_1 and I_2 are derived as follows:

$$I_1 = \frac{(R_2 + R_L)V_1 - R_LV_2}{R_1R_2 + R_1R_L + R_2R_L} \quad (3)$$

$$I_2 = \frac{(R_1 + R_L)V_2 - R_LV_1}{R_1R_2 + R_1R_L + R_2R_L} \quad (4)$$

Circulating current phenomena mainly depend on the converter output voltages [25], expressed as

$$I_{C12} = -I_{C21} = \frac{V_1 - V_2}{R_1 + R_2} \quad (5)$$

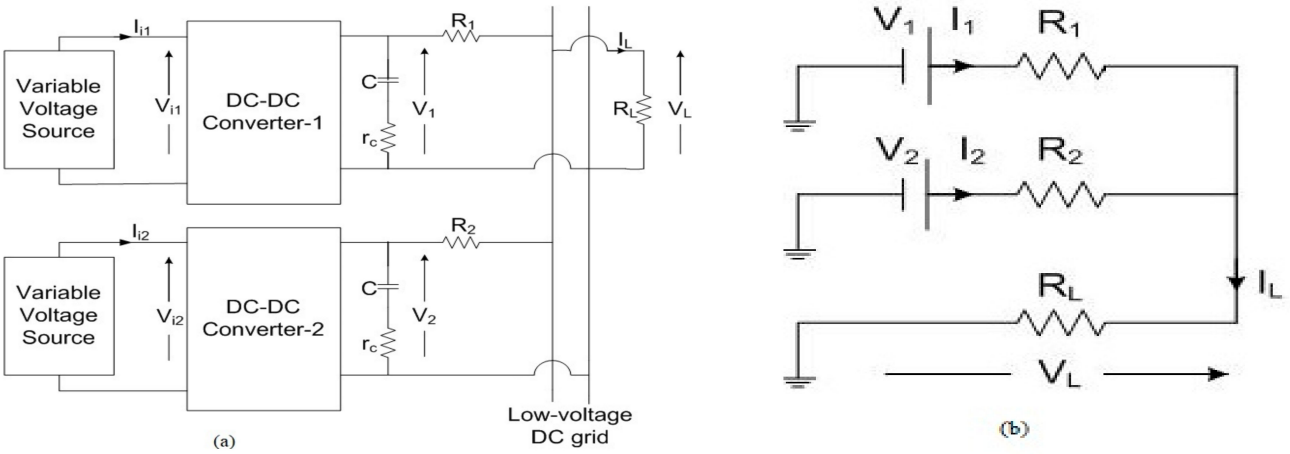

Figure 2. (**a**) Parallel DC–DC buck converter. (**b**) Equivalent circuit.

3. Voltage Control by Adding R_{droop}

The converter current sharing with the addition of a series resistor R_{droop} is explained below and shown in Figure 3a, which is similar to Figure 2a but with the addition of a series resistor R_{droop} in each converter.

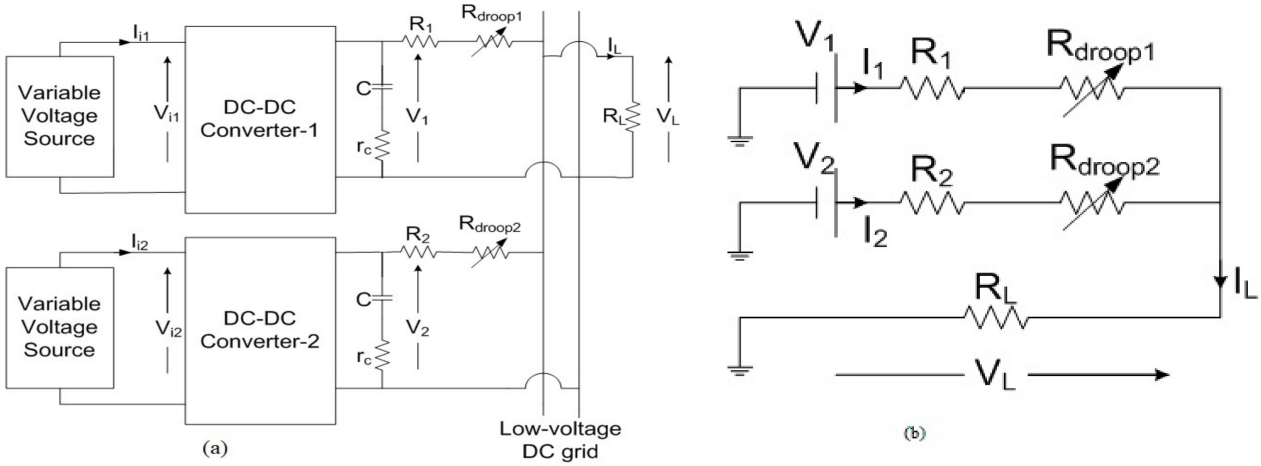

Figure 3. (**a**) Parallel DC–DC buck converter with R_{droop}. (**b**) Equivalent circuit.

Applying KVL to the circuit in Figure 3b, the following equations are obtained

$$V_1 - I_1(R_1 + R_{droop1}) - I_L R_L = 0 \quad (6)$$

$$V_2 - I_2(R_2 + R_{droop2}) - I_L R_L = 0 \quad (7)$$

The equivalent circuit of the parallel connection of the DC–DC buck converter with R_{droop} is shown in Figure 3b.

By using Equations (6) and (7), the derived converter output currents I_1 and I_2 are given as

$$I_1 = \frac{\left(R_2 + R_{droop2} + R_L\right)V_1 - R_L V_2}{(R_1 + R_{droop1})(R_2 + R_{droop2}) + (R_1 + R_{droop1})R_L + (R_2 + R_{droop2})R_L} \quad (8)$$

$$I_2 = \frac{\left(R_1 + R_{droop1} + R_L\right)V_2 - R_L V_1}{(R_1 + R_{droop1})(R_2 + R_{droop2}) + (R_1 + R_{droop1})R_L + (R_2 + R_{droop2})R_L} \quad (9)$$

Circulating current is given as

$$I_{C12} = -I_{C21} = \frac{V_1 - V_2}{R_1 + R_{droop1} + R_2 + R_{droop2}} \quad (10)$$

The two considered parallel converters with the proposed virtual droop resistance method are shown in Figure 4. The output current from each converter 1 and 2 was taken as the feedback and multiplied with the calculated R_{droop1} and R_{droop2} values. The cable resistances were considered as R_{c1} and R_{c2}. From the reference voltage V_{ref}, subtracting the resultant signal produces a new reference signal (V^*_{refj}), giving a generalized equation as

$$V^*_{refj} = V_{ref} - I_j * R_{droopj} \qquad \text{where } j = 1, 2, \ldots, n \quad (11)$$

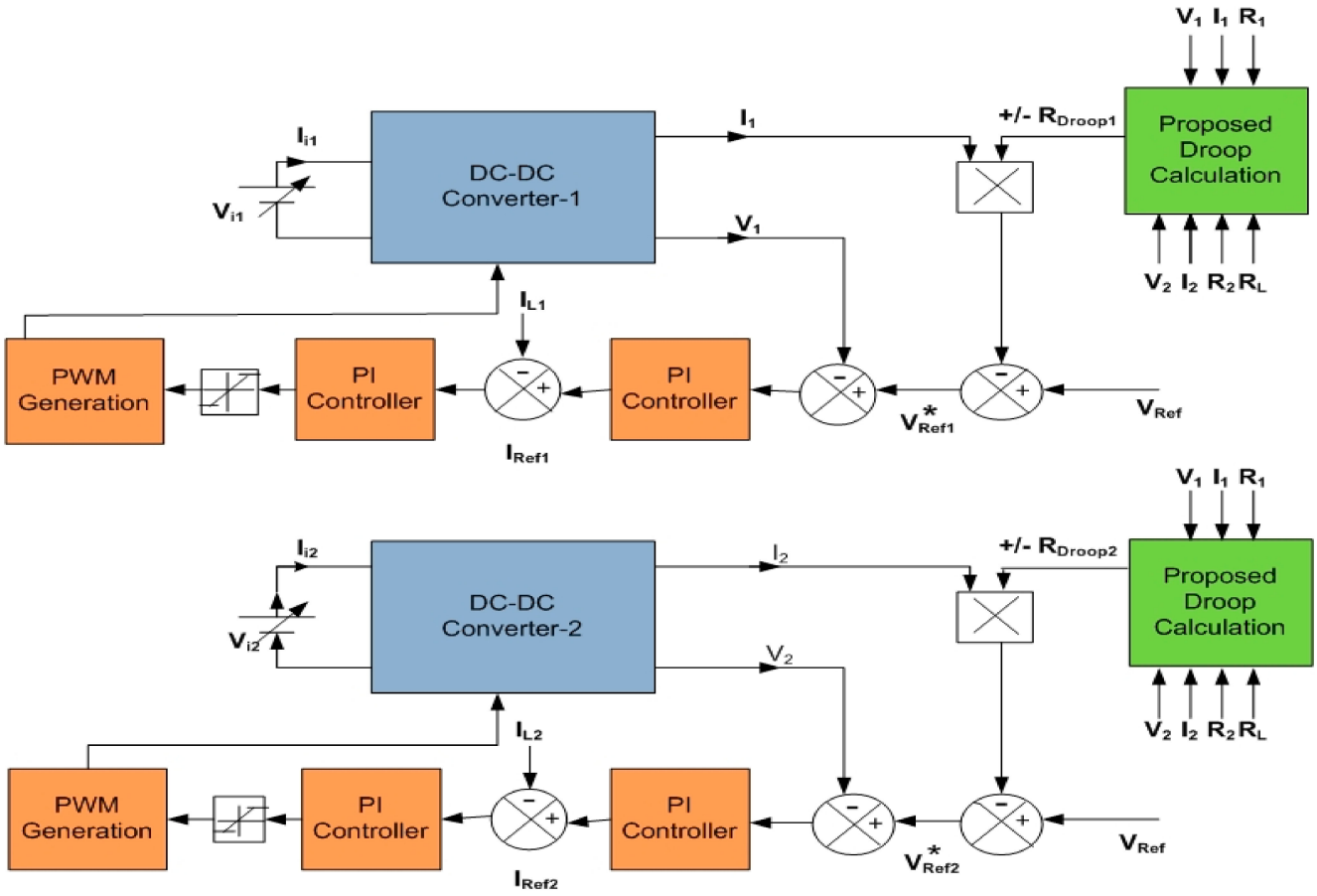

Figure 4. Control diagram of parallel converters with R_{droop}.

4. Proposed Adaptive Droop Control Strategy

A pictorial representation of the proposed droop resistance calculation considering two parallel converters is shown in Figure 5. The input parameters are the voltages and currents of converter 1 and converter 2, reference voltage, cable resistances R_1 and R_2, load resistance R_L, droop resistance R_{droop}, and delta resistance R_{delta}. Converter 1 Power P_1 and Converter 2 Power P_2 were calculated using the input parameters. The calculated droop resistance values R_{droop1} and R_{droop2} from the proposed strategy are used in the control diagram shown in Figure 4.

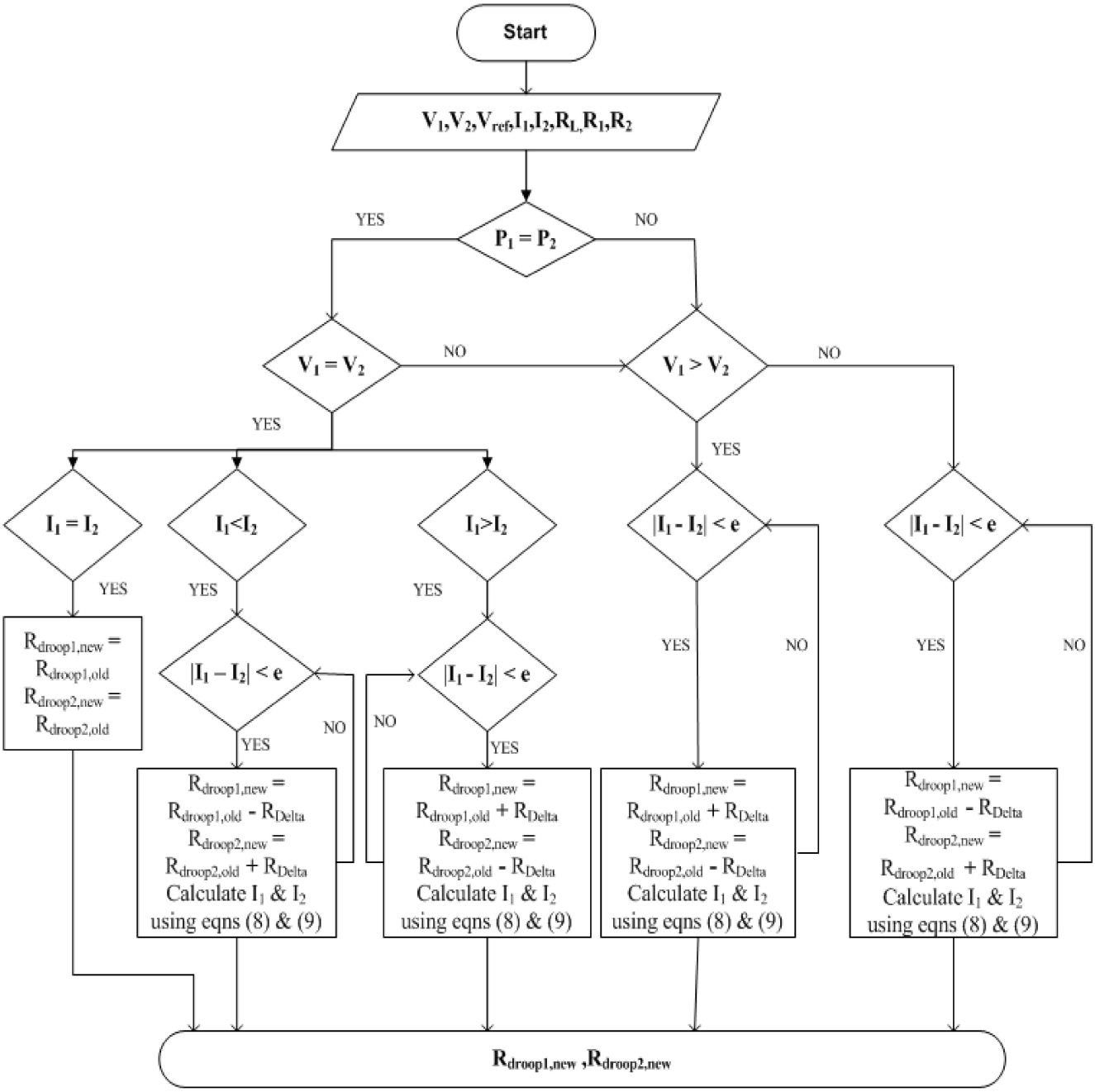

Figure 5. Proposed drop control flowchart.

Whenever any change occurs in the source voltage, load, or cable resistance, the current sharing of converters will become unequal. A maximum voltage deviation is caused when one converter has a lower current sharing and others have a higher current sharing. The power, voltage, and current of both converters are validated. In the case of both the converter currents $\mathbf{I}_1$ and $\mathbf{I}_2$ being the same, no circulating current flows between the converters and there is no requirement to adjust the droop resistance and consider new droop resistances as the old droop resistances shown in Equations (12) and (13).

$$R_{droop1,new} = R_{droop1,old} \quad (12)$$

$$R_{droop2,new} = R_{droop2,old} \quad (13)$$

When converter current $\mathbf{I}_1$ is more than $\mathbf{I}_2$, there will be circulating current $\mathbf{I}_{C12}$ flowing between converter 1 and converter 2. To reduce the circulating current effect, the droop resistances are adjusted by using Equations (14) and (15).

$$R_{droop1,new} = R_{droop1,old} + R_{delta} \quad (14)$$

$$R_{droop2,new} = R_{droop2,old} - R_{delta} \quad (15)$$

The calculated values of currents using Equations (8) and (9) are again verified to be within allowable limits, and the flow of adjusting droop resistances will continue until the criteria are satisfied.

Similarly, when converter current $\mathbf{I}_1$ is less than $\mathbf{I}_2$, there will be circulating current $\mathbf{I}_{C21}$ flowing between converter 2 and converter 1. To reduce the circulating current effect, the droop resistances are adjusted by using Equations (16) and (17).

$$R_{droop1,new} = R_{droop1,old} - R_{delta} \quad (16)$$

$$R_{droop2,new} = R_{droop2,old} + R_{delta} \quad (17)$$

The calculated values of currents $\mathbf{I}_1$ and $\mathbf{I}_2$ using Equations (8) and (9) are again verified to be within allowable limits and are continued until the criteria are satisfied. During unequal converter voltages $\mathbf{V}_1$ and $\mathbf{V}_2$, a similar procedure is followed such as validating currents and adjusting droop resistances accordingly.

The adaptive droop control method will dynamically adjust according to the variations in parameters and will maintain the circulating current phenomena within the desirable limits. The proposed strategy was considered and applied only to two parallel source converters in this paper. This method is adaptable to the change in source voltage, load variations, change in cable resistances, etc. It also gives better current sharing with minimal circulating currents. Moreover, the controller responds fast, as the computation involved is less. This shows the robustness of the controller.

5. Results and Discussion

The proposed model was analyzed with different cases by considering different scenarios of source voltage, load, and cable resistance. The effectiveness of the proposed control method is shown by comparing the results with the basic model and novel droop control [21]. The proposed algorithm was carried out considering two parallel dc–dc buck converters and simulated using MATLAB/SIMULINK. The results of the simulated model compared with HIL Simulator show the effectiveness of the controller in real-time. The system parameters considered are given in Table 2.

Table 2. Nominal parameters of buck converter.

Parameters	Symbol	Value
Input Voltage	V_{in}	100 V
Output Voltage	V_{out}	48 V
Output Power	P_{out}	96 W
Filter Inductor	L	12.48 mH
ESR of the filter inductor	r_l	0.002 Ω
Filter capacitor	C	10.41 μF
ESR of the filter capacitor	r_c	0.03 Ω
Nominal switching frequency	f_{sw}	10 kHz

5.1. Simulation Results

The robustness of the proposed droop control method was considered with combinations of different cable resistances, varying source voltages, and load variations considered at different intervals, as mentioned in Tables 3–5.

Table 3. Different cable resistances.

Parameter	Value
Cable Resistance of Converter 1	100 mΩ
Cable Resistance of Converter 2	150 mΩ

Table 4. Load variations at different intervals.

Time (s) →	0–1	1–2	2–3.5	3.5–4
Load (W)	192 W	192 W	144 W	192 W

Table 5. Variation in source voltage of converters at different intervals.

Time (s) →	0–1	1–2	2–3	3–4
Source Voltage of Converter 1 (V)	100 V	100 V	110 V	100 V
Source Voltage of Converter 2 (V)	100 V	110 V	100 V	100 V

5.1.1. Without Droop Control

Case 1: Different cable resistances

Considering the source voltage of converter 1 and 2 as 100 V, the resistive load was 192 W and the different cable resistances were as shown in Table 3. Figure 6 shows the results of $\mathbf{V_L}$, $\mathbf{I_L}$, and the current sharing of converters $\mathbf{I}_1$ and $\mathbf{I}_2$. The load voltage was 47.75 V and the load current was 4 A, with a current share of 2.4 A and 1.6 A of converter 1 and 2, respectively. The current sharing error $\mathbf{I}_{err}$ was 20% and the circulating current $\mathbf{I}_{cir}$ was 0.4 A.

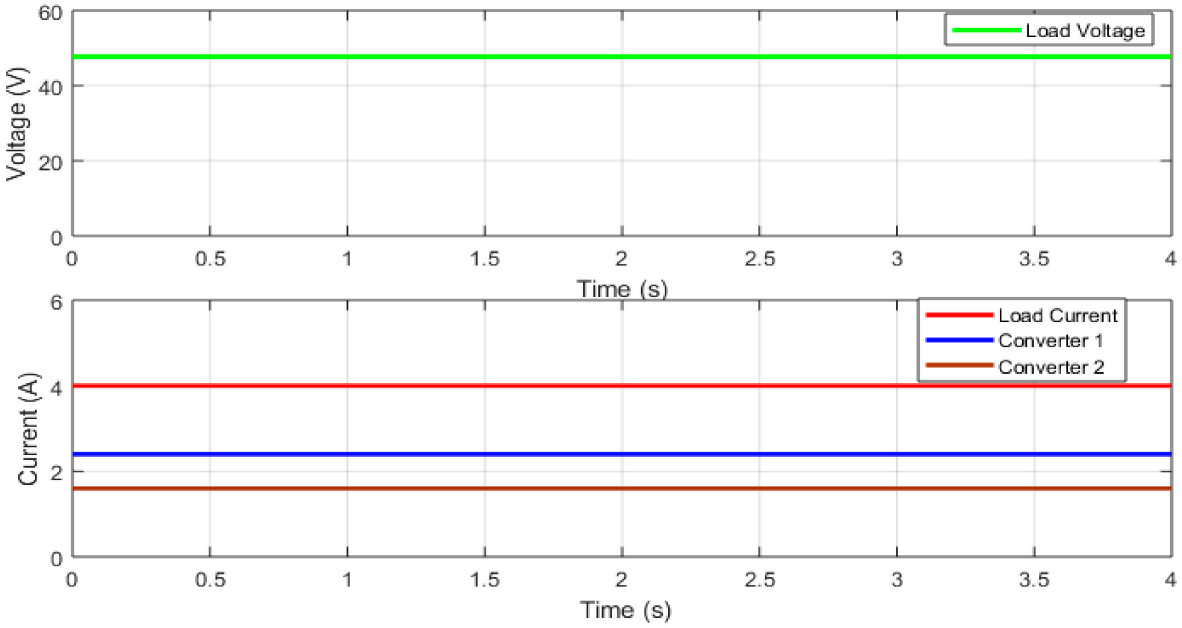

Figure 6. Simulation results for different cable resistances without any droop control: load voltage, converter output currents and load current.

Case 2: Variation in load with different cable resistances

Considering the source voltage of converters 1 and 2 as 100 V, the variation in resistive load was as shown in Table 4 and the different cable resistances were as shown in Table 3. Figure 7 shows the results of $\mathbf{V_L}$, $\mathbf{I_L}$, and the current sharing of converters $\mathbf{I}_1$ and $\mathbf{I}_2$. The load voltage was 47.75 V and the load current was 4 A with a current share of 2.4 A and 1.6 A of converter 1 and 2, respectively. During 2–3.5 s, the load changed to 144 W, the load voltage was 47.75 V, and the load current was 3 A with a current share of 1.81 A and 1.19 A of converter 1 and 2, respectively. The current sharing error $\mathbf{I}_{err}$ was 20.6% and the circulating current $\mathbf{I}_{cir}$ was 0.31 A.

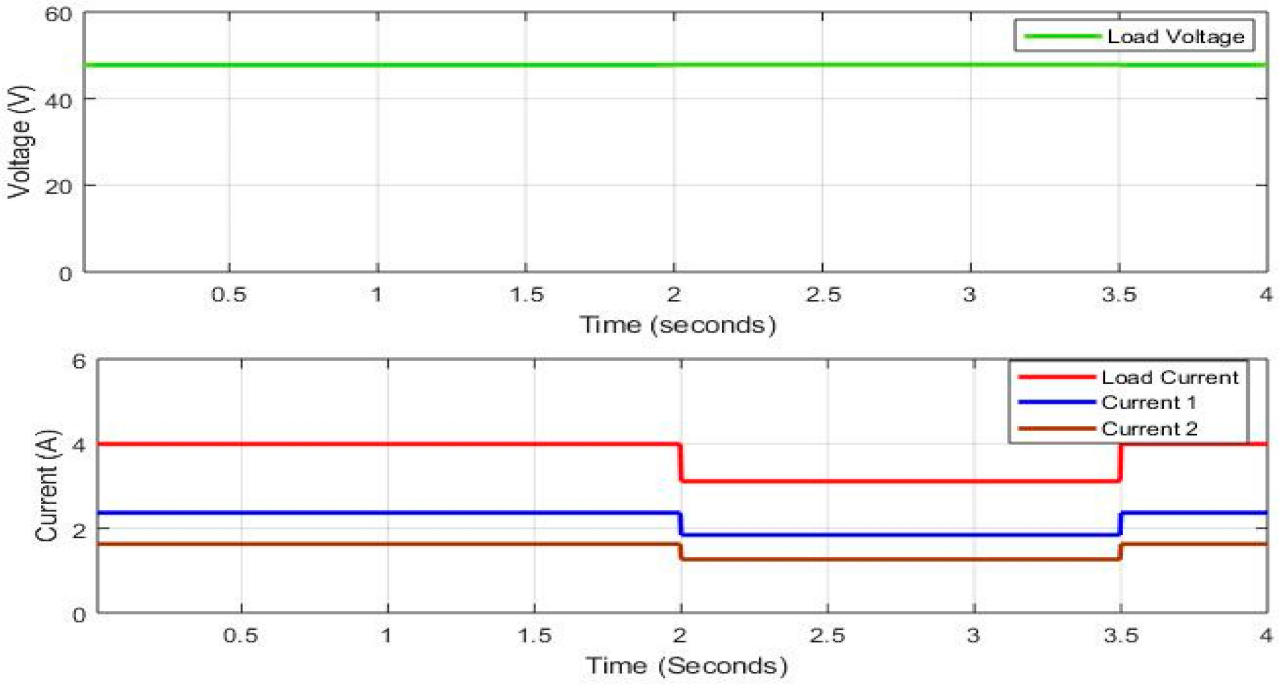

Figure 7. Simulation results for variation in load with different cable resistances without any droop control: load voltage, converter output currents and load current.

Case 3: Variation in source voltage and load with different cable resistances

Considering the variation in source voltage, as shown in Table 5, the variation in resistive load was as shown in Table 4 and the different cable resistances were as shown in Table 3. Figure 8 shows the results of $\mathbf{V_L}$, $\mathbf{I_L}$, and the current sharing of converters $\mathbf{I}_1$ and $\mathbf{I}_2$. During 2–3 s, the load voltage was 47.8 V and the load current was 3 A with a current share of 1.95 A and 1.05 A of converter 1 and 2, respectively. The current sharing error $\mathbf{I}_{err}$ was 30% and the circulating current $\mathbf{I}_{cir}$ was 0.45 A.

5.1.2. Novel Droop Control

Case 1: Different cable resistances

Considering the source voltages of converter 1 and 2 as 100 V, the resistive load was 192 W and the different cable resistances was as shown in Table 3. Figure 9 shows the results of $\mathbf{V_L}$, $\mathbf{I_L}$, and the current sharing of converters $\mathbf{I}_1$ and $\mathbf{I}_2$. The load voltage was 46.3 V and the load current was 4 A with a current share of 2.2 A and 1.8 A of converter 1 and 2, respectively. The current sharing error $\mathbf{I}_{err}$ was 10% and the circulating current $\mathbf{I}_{cir}$ was 0.2 A.

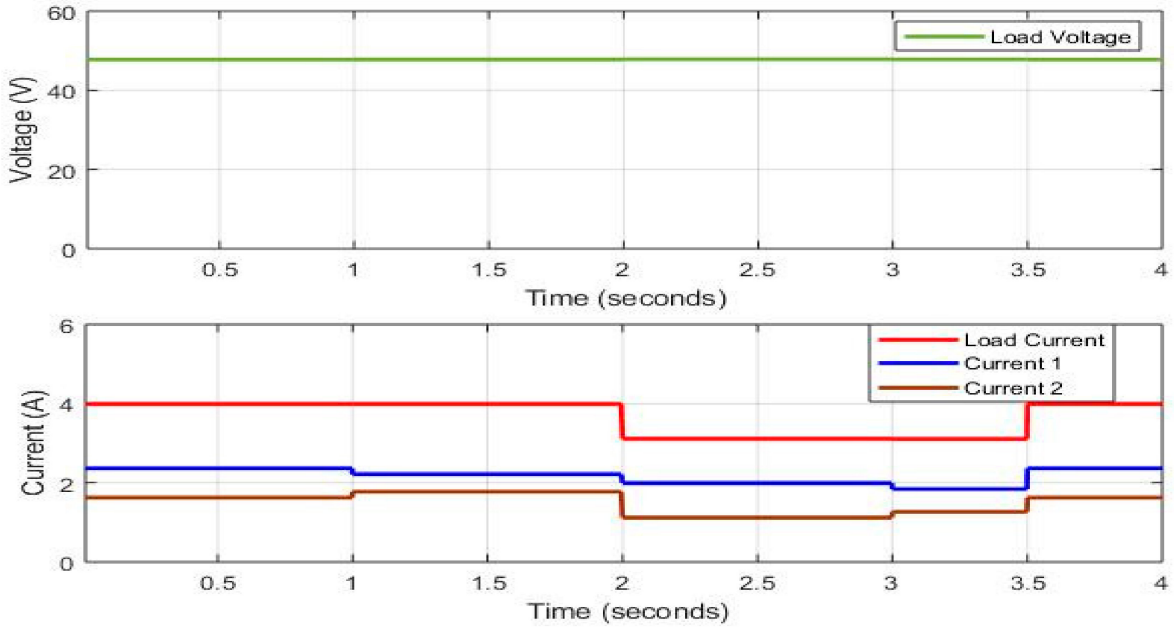

Figure 8. Simulation results for variation in source voltage and load with different cable resistances without any droop control: load voltage, converter output currents and load current.

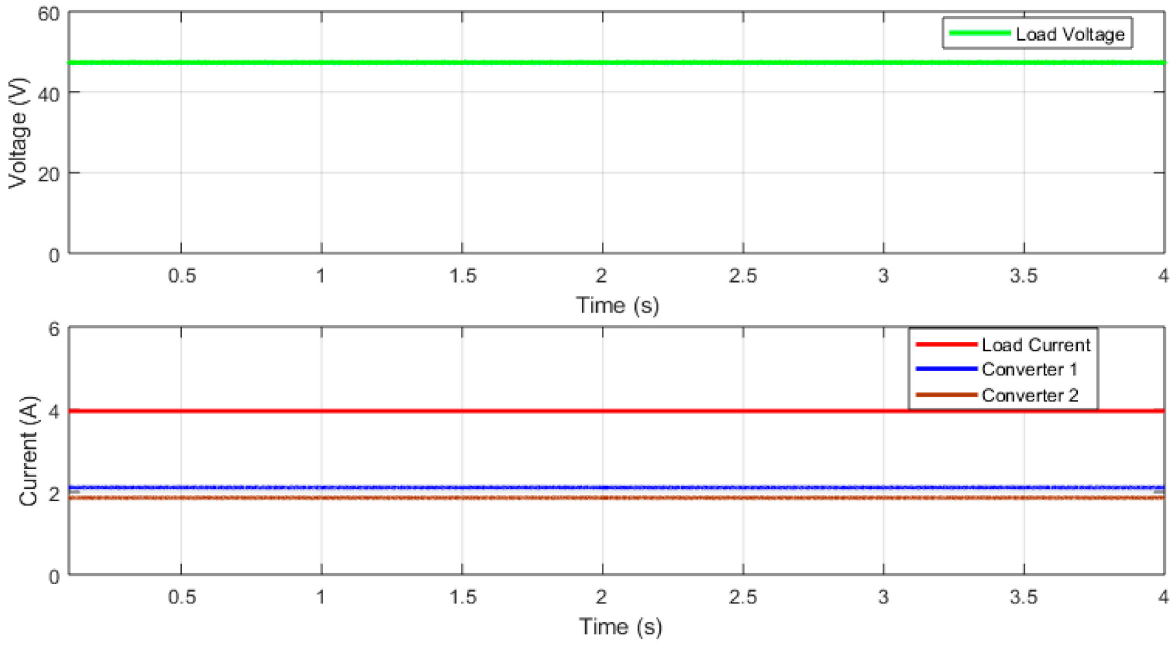

Figure 9. Simulation results for different cable resistance for novel droop control: load voltage, converter output currents and load current.

Case 2: Variation in load with different cable resistances

Considering the source voltage of converters 1 and 2 as 100 V, the variation in resistive load was as shown in Table 4 and the different cable resistances were as shown in Table 3. Figure 10 shows the results of $\mathbf{V_L}$, $\mathbf{I_L}$, and the current sharing of converters $\mathbf{I}_1$ and $\mathbf{I}_2$.

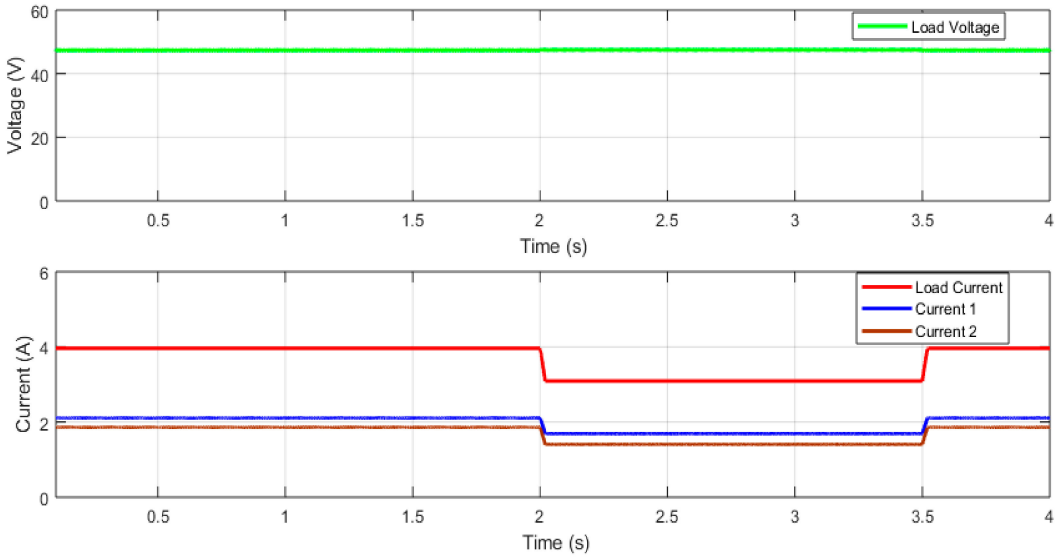

Figure 10. Simulation results for variation in load with different cable resistances for novel droop control: load voltage, converter output currents and load current.

The load voltage was 46.3 V and the load current was 4 A with a current share of 2.2 A and 1.8 A of converter 1 and 2, respectively. During 2–3.5 s, the load changed to 144 W, the load voltage was 46.4 V, and the load current was 3 A with a current share of 1.67 A and 1.33 A of converter 1 and 2, respectively. The current sharing error $\mathbf{I}_{err}$ was 11.3% and the circulating current $\mathbf{I}_{cir}$ was 0.17 A.

Case 3: Variation in source voltage and load with different cable resistances

Considering the variation in source voltage, as shown in Table 5, the variation in resistive load was as shown in Table 4 and the different cable resistances were as shown in Table 3. Figure 11 shows the results of $\mathbf{V_L}$, $\mathbf{I_L}$, and the current sharing of converters $\mathbf{I}_1$ and $\mathbf{I}_2$. During 2–3 s, the load voltage was 46.5 V and the load current was 3 A with a current share of 1.75 A and 1.25 A of converter 1 and 2, respectively. The current sharing error $\mathbf{I}_{err}$ was 16.6% and the circulating current $\mathbf{I}_{cir}$ was 0.25 A.

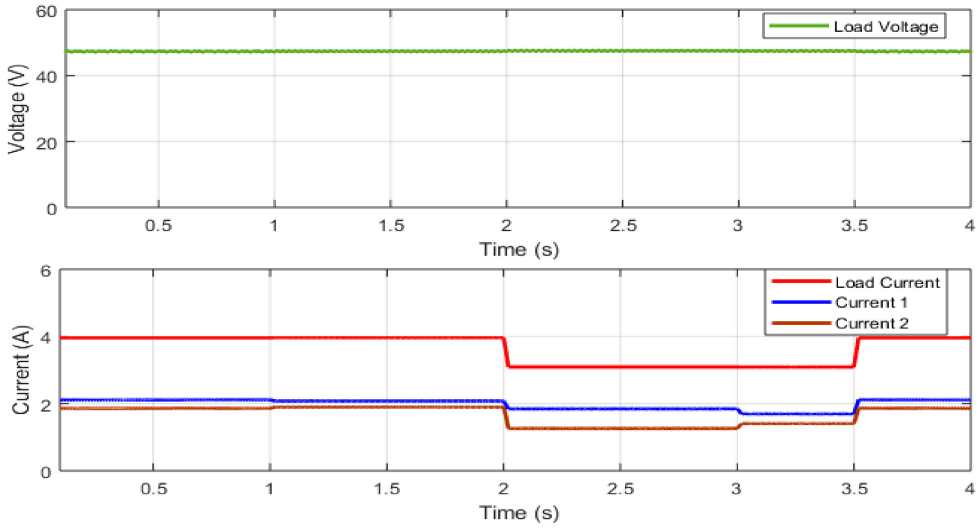

Figure 11. Simulation results for variation in source voltage and load with different cable resistances for novel droop control: load voltage, converter output currents and load current.

5.1.3. Proposed Droop Control

Case 1: Different cable resistances

Considering the source voltages of converter 1 and 2 as 100 V, the resistive load was 192 W and the different cable resistances were as shown in Table 3. Figure 12 shows the results of $\mathbf{V_L}$, $\mathbf{I_L}$, and the current sharing of converters $\mathbf{I}_1$ and $\mathbf{I}_2$. The load voltage was 47.8 V and the load current was 4 A with a current share of 2.02 A and 1.98 A of converter 1 and 2, respectively. The current sharing error $\mathbf{I}_{err}$ was 1% and the circulating current $\mathbf{I}_{cir}$ was 0.02 A. There were minute adjustments in the current sharing of converters $\mathbf{I}_1$ and $\mathbf{I}_2$ due to the dynamic droop control.

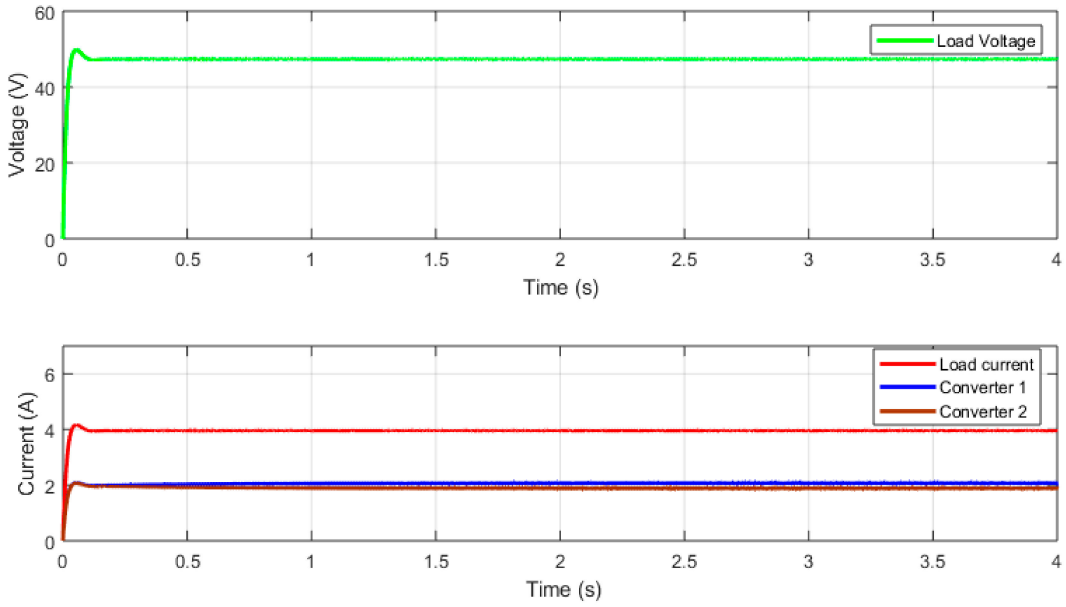

Figure 12. Simulation results for different cable resistances for proposed droop control: load voltage, converter output currents and load current.

Case 2: Variation in load with different cable resistances

Considering the source voltages of converters 1 and 2 as 100 V, the variation in resistive load was as shown in Table 4 and the different cable resistances were as shown in Table 3. Figure 13 shows the results of $\mathbf{V_L}$, $\mathbf{I_L}$, and the current sharing of converters $\mathbf{I}_1$ and $\mathbf{I}_2$. The load voltage was 47.8 V and the load current was 4 A with a current share of 2.02 A and 1.98 A of converter 1 and 2, respectively. During 2–3.5 s, the load changed to 144 W, the load voltage was 47.8 V, and the load current was 3 A with a current share of 1.516 A and 1.484 A of converter 1 and 2, respectively. The current sharing error $\mathbf{I}_{err}$ was 1.06% and the circulating current $\mathbf{I}_{cir}$ was 0.016 A. There were minute adjustments in the current sharing of converters $\mathbf{I}_1$ and $\mathbf{I}_2$ due to the dynamic droop control.

Case 3: Variation in source voltage and load with different cable resistances

Considering the variation in source voltage, as shown in Table 5, the variation in resistive load was as shown in Table 4 and the different cable resistances were as shown in Table 3. Figure 14 shows the results of $\mathbf{V_L}$, $\mathbf{I_L}$, and the current sharing of converters $\mathbf{I}_1$ and $\mathbf{I}_2$. During 2–3 s, the load voltage was 47.8 V and the load current was 3 A with a current share of 1.54 A and 1.46 A of converter 1 and 2, respectively. The current sharing error $\mathbf{I}_{err}$ was 2.6% and the circulating current $\mathbf{I}_{cir}$ was 0.04 A. There were minute adjustments in the current sharing of converters $\mathbf{I}_1$ and $\mathbf{I}_2$ due to the dynamic droop control.

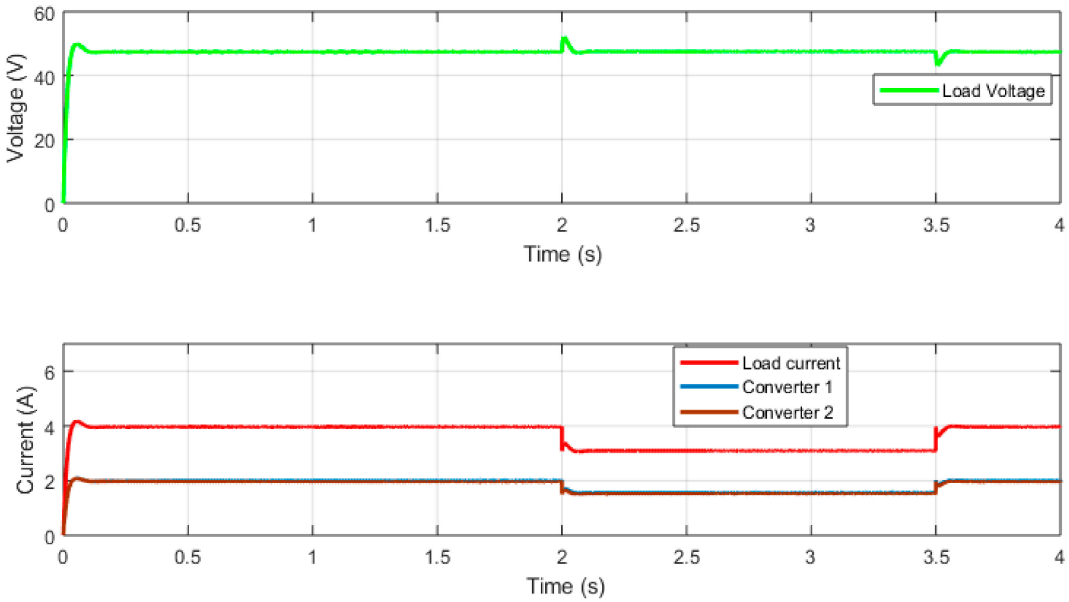

Figure 13. Simulation results for variation in load with different cable resistances for proposed droop control: load voltage, converter output currents and load current.

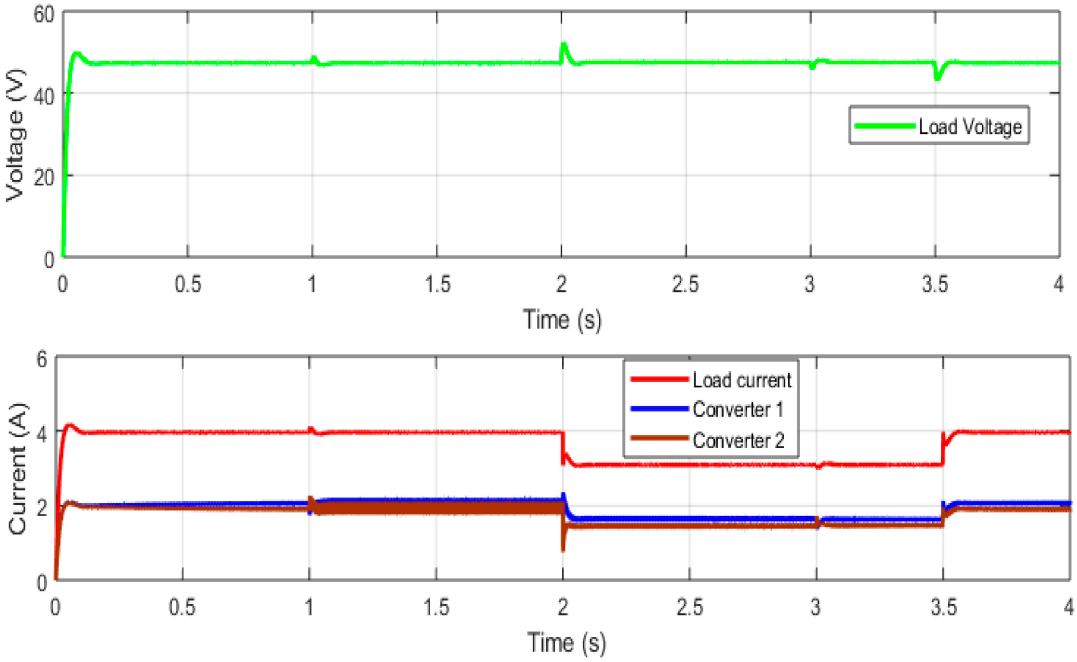

Figure 14. Simulation results for variation in source voltage and load with different cable resistances for proposed droop control: load voltage, converter output currents and load current.

5.2. Experimental Validation

A Hardware-In-Loop (HIL) real-time simulator OPAL-RT-OP4510 was used to verify the effectiveness of the proposed method shown in Figure 15. We also considered the same parameters analyzed with the simulation model of MATLAB/SIMULINK.

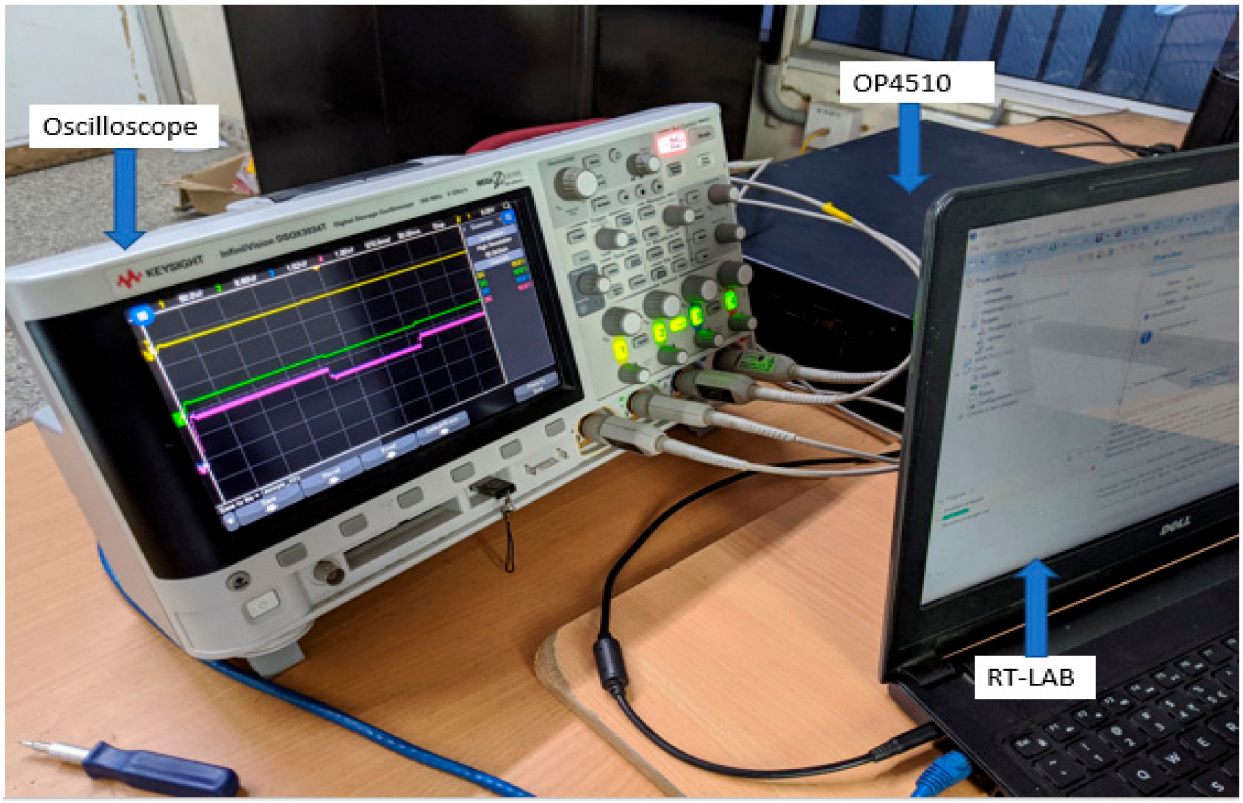

Figure 15. HIL real-time simulator setup.

5.2.1. Novel Droop Control

Case 1: Different cable resistances

Considering the same parameter values as in case 1 of the simulation, Section 5.1.2., the experimental results of $\mathbf{V_L}$, $\mathbf{I_L}$, $\mathbf{I}_1$, and $\mathbf{I}_2$ are shown in Figure 16, which were similar to those in Figure 9. The load voltage was 46.0 V and the load current was 4 A with a current share of 2.24 A and 1.76 A of converter 1 and 2, respectively. The current sharing error $\mathbf{I}_{err}$ was 12% and the circulating current $\mathbf{I}_{cir}$ was 0.24 A.

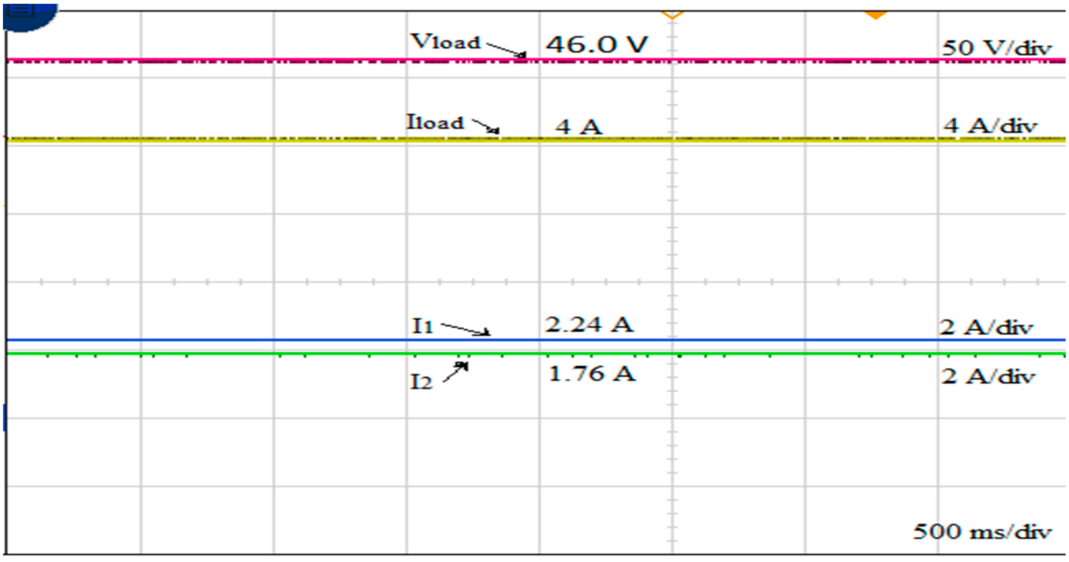

Figure 16. Experimental results for different cable resistances for the novel droop control.

Case 2: Variation in load with different cable resistances

Considering the same parameter values as in case 2 of the simulation, Section 5.1.2., the experimental results of $\mathbf{V_L}$, $\mathbf{I_L}$, $\mathbf{I}_1$, and $\mathbf{I}_2$ are shown in Figure 17, which were similar to those in Figure 10. The load voltage was 46.3 V and the load current was 4 A with a current share of 2.24 A and 1.76 A of converter 1 and 2, respectively. During 2–3.5 s, the load changed to 144 W, the load voltage was 46.1 V, and the load current was 3 A with a current share of 1.69 A and 1.31 A of converter 1 and 2, respectively. The current sharing error $\mathbf{I}_{err}$ was 12.6% and the circulating current $\mathbf{I}_{cir}$ was 0.19 A.

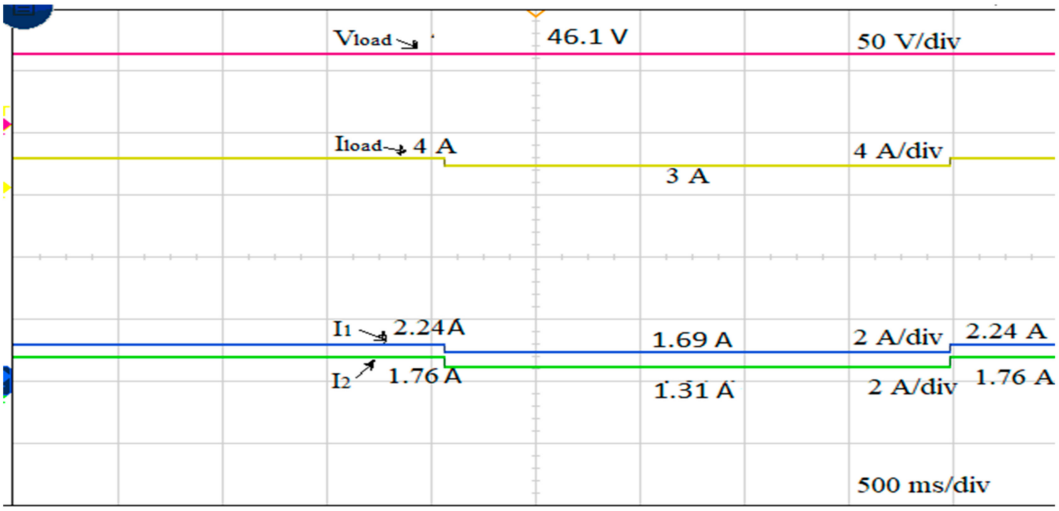

Figure 17. Experimental results for variation in load with different cable resistances for the novel droop control.

Case 3: Variation in source voltage and load with different cable resistances

Considering the same parameter values as in case 3 of the simulation, Section 5.1.2., the experimental results of $\mathbf{V_L}$, $\mathbf{I_L}$, $\mathbf{I}_1$, and $\mathbf{I}_2$ are shown in Figure 18, which were similar to those in Figure 11. During 2–3 s, the load voltage was 46.4 V and the load current was 3 A with a current share of 1.8 A and 1.2 A of converter 1 and 2, respectively. The current sharing error $\mathbf{I}_{err}$ was 20% and the circulating current $\mathbf{I}_{cir}$ was 0.3 A.

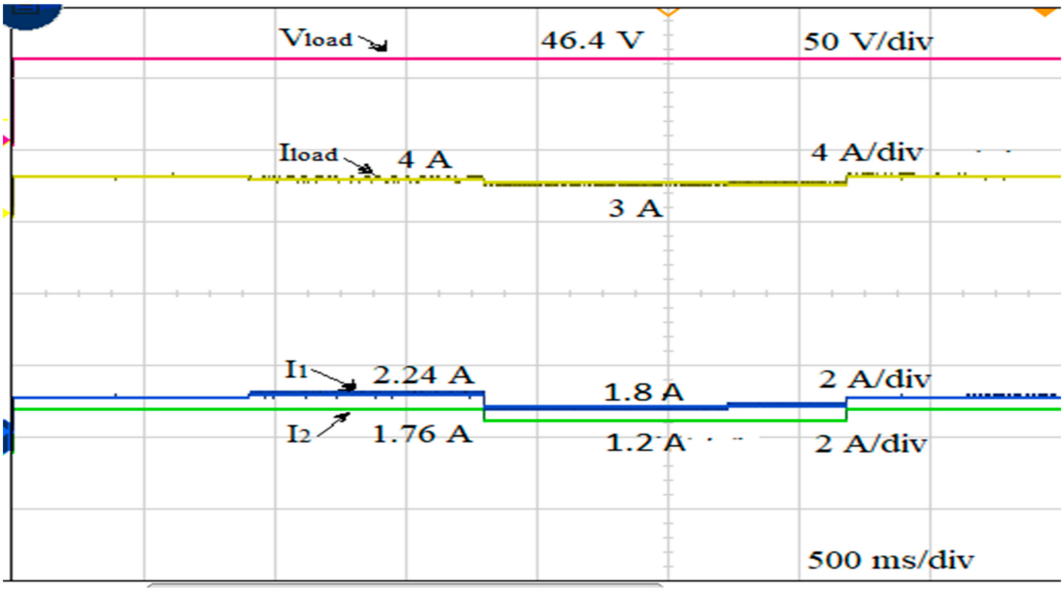

Figure 18. Experimental results for variation in source voltage and load with different cable resistances for the novel droop control.

5.2.2. Proposed Droop Control

Case 1: Different cable resistances

Considering the same parameter values as in case 1 of the simulation, Section 5.1.3., the experimental results of $\mathbf{V_L}$, $\mathbf{I_L}$, $\mathbf{I}_1$, and $\mathbf{I}_2$ are shown in Figure 19, which were similar to those in Figure 12. The load voltage was 47.7 V and the load current was 4 A with a current share of 2.06 A and 1.94 A of converter 1 and 2, respectively. The current sharing error $\mathbf{I}_{err}$ was 3% and the circulating current $\mathbf{I}_{cir}$ was 0.06 A. There were minute adjustments in the current sharing of converters $\mathbf{I}_1$ and $\mathbf{I}_2$ due to the dynamic droop control.

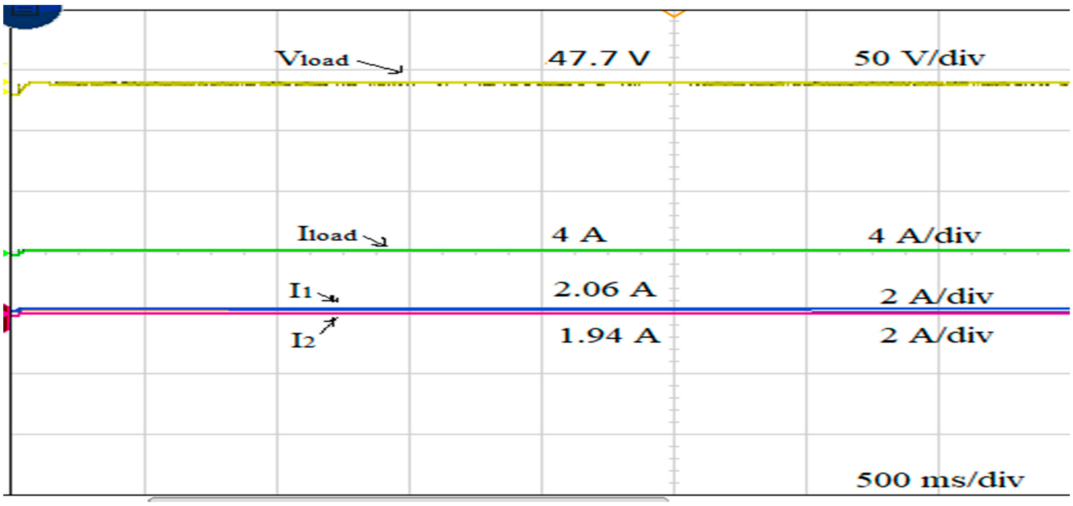

Figure 19. Experimental results for different cable resistances for proposed droop control.

Case 2: Variation in load with different cable resistances

Considering the same parameter values as in case 2 of the simulation, Section 5.1.3., the experimental results of $\mathbf{V_L}$, $\mathbf{I_L}$, $\mathbf{I}_1$, and $\mathbf{I}_2$ are shown in Figure 20, which were similar to those in Figure 13. The load voltage was 47.7 V and the load current was 4 A with a current share of 2.06 A and 1.94 A of converter 1 and 2, respectively. During 2–3.5 s, the load changed to 144 W, the load voltage was 47.8 V, and the load current was 3 A with a current share of 1.55 A and 1.45 A of converter 1 and 2, respectively. The current sharing error $\mathbf{I}_{err}$ was 3.3% and the circulating current $\mathbf{I}_{cir}$ was 0.05 A. There were minute adjustments in the current sharing of converters $\mathbf{I}_1$ and $\mathbf{I}_2$ due to the dynamic droop control.

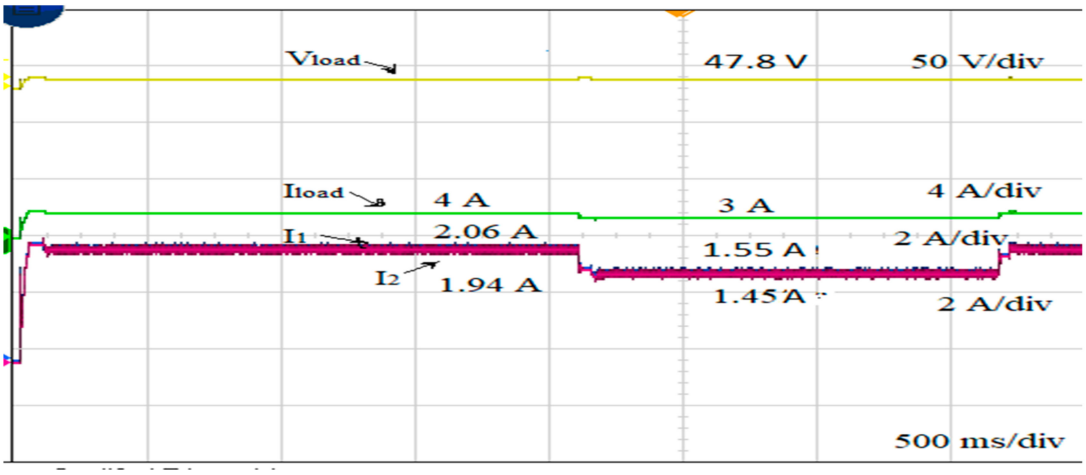

Figure 20. Experimental results for variation in load with different cable resistances for proposed droop control.

Case 3: Variation in source voltage and load with different cable resistances

Considering the same parameter values as in case 2 of the simulation, Section 5.1.3., the experimental results of $\mathbf{V_L}$, $\mathbf{I_L}$, $\mathbf{I}_1$, and $\mathbf{I}_2$ are shown in Figure 21, which were similar to those in Figure 13. The load voltage was 47.7 V and the load current was 4 A with a current share of 2.06 A and 1.94 A of converter 1 and 2, respectively. During 2–3.5 s, the load changed to 144 W, the load voltage was 47.8 V, and the load current was 3 A with a current share of 1.55 A and 1.45 A of converter 1 and 2, respectively. The current sharing error $\mathbf{I}_{err}$ was 3.3% and the circulating current $\mathbf{I}_{cir}$ was 0.05 A. There were minute adjustments in the current sharing of converters $\mathbf{I}_1$ and $\mathbf{I}_2$ due to the dynamic droop control.

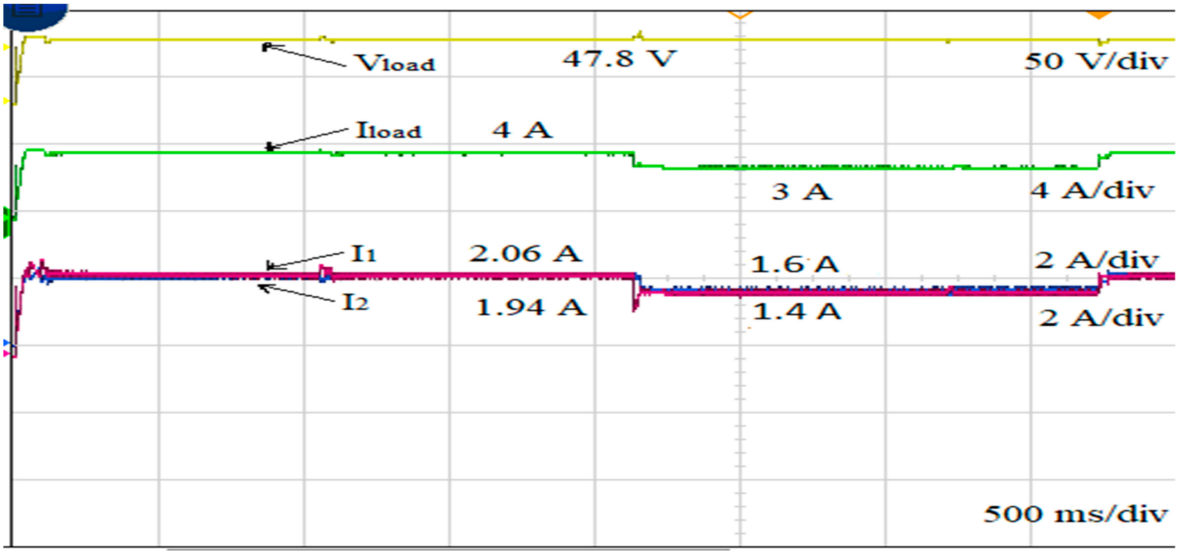

Figure 21. Experimental results for variation in source voltage and load with different cable resistances for proposed droop control.

The simulation results of the load sharing error and circulating current for different cable resistance conditions are given in Table 6, the varying loads with different cable resistances are given in Table 7, and the varying source voltages and loads with different cable resistances are given in Table 8.

Table 6. Comparison of simulation results of different methods considering different cable resistances.

Method	$\mathbf{V_L}$ (V)	$\mathbf{I_L}$ ($\mathbf{I_1}$, $\mathbf{I_2}$) (A)	I_{Error} (%)	$\lvert\mathbf{I}_{Cir}\rvert$ (A)
Without Droop Control	47.75	4 (2.4, 1.6)	20	0.4
Novel Droop Control [21]	46.3	4 (2.2, 1.8)	10	0.2
Proposed Droop Control	47.8	4 (2.02, 1.98)	1	0.02

Table 7. Comparison of simulation results of different methods considering variation in load with different cable resistances.

Method	$\mathbf{V_L}$ (V)	$\mathbf{I_L}$ ($\mathbf{I_1}$, $\mathbf{I_2}$) (A)	I_{Error} (%)	$\lvert\mathbf{I}_{Cir}\rvert$ (A)
Without Droop Control	47.75	3 (1.81, 1.19)	20.6	0.31
Novel Droop Control [21]	46.4	3 (1.67, 1.33)	11.3	0.17
Proposed Droop Control	47.8	3 (1.516, 1.484)	1.06	0.016

Table 8. Comparison of simulation results of different methods considering variation in source voltage and load with different cable resistances.

Method	V_L (V)	I_L (I_1, I_2) (A)	I_{Error} (%)	$\|I_{Cir}\|$ (A)
Without Droop Control	47.8	3 (1.95, 1.05)	30	0.45
Novel Droop Control [21]	46.5	3 (1.75, 1.25)	16.6	0.25
Proposed Droop Control	47.8	3 (1.54, 1.46)	2.6	0.04

The experimental results of the load sharing error and circulating current for different cable resistance conditions are given in Table 9, the varying loads with different cable resistances are given in Table 10, and the varying source voltages and loads with different cable resistances are given in Table 11. It is clearly shown with the proposed droop control method that the load sharing error reduced and minimized the circulating current due to dynamic droop resistance.

Table 9. Comparison of experimental results of different methods considering different cable resistances.

Method	V_L (V)	I_L (I_1, I_2) (A)	I_{Error} (%)	$\|I_{Cir}\|$ (A)
Novel Droop Control [21]	46.0	4 (2.24, 1.76)	12	0.24
Proposed Droop Control	47.7	4 (2.06, 1.94)	3	0.06

Table 10. Comparison of experimental results of different methods considering variation in load with different cable resistances.

Method	V_L (V)	I_L (I_1, I_2) (A)	I_{Error} (%)	$\|I_{Cir}\|$ (A)
Novel Droop Control [21]	46.1	3 (1.69, 1.31)	12.6	0.19
Proposed Droop Control	47.8	3 (1.55, 1.45)	3.3	0.05

Table 11. Comparison of experimental results of different methods considering variation in source voltage and load with different cable resistances.

Method	V_L (V)	I_L (I_1, I_2) (A)	I_{Error} (%)	$\|I_{Cir}\|$ (A)
Novel Droop Control [21]	46.4	3 (1.8, 1.2)	20	0.3
Proposed Droop Control	47.8	3 (1.6, 1.4)	6.6	0.1

The simulation and experimental results of the proposed adaptive droop control considering different cable resistance conditions are given in Table 12, the varying loads and different cable resistances are given in Table 13, and the varying source voltages and loads with different cable resistances are given in Table 14.

Table 12. Comparison of simulation and experimental results of the proposed adaptive droop control for different cable resistances.

Method	V_L (V)	I_L (I_1, I_2) (A)	I_{Error} (%)	$\|I_{Cir}\|$ (A)
Simulation	47.8	4 (2.02, 1.98)	1	0.02
Experimental	47.7	4 (2.06, 1.94)	3	0.06

Table 13. Comparison of simulation and experimental results of proposed adaptive droop control for varying load and different cable resistances.

Method	V_L (V)	I_L (I_1, I_2) (A)	I_{Error} (%)	$\|I_{Cir}\|$ (A)
Simulation	47.8	3 (1.516, 1.484)	1.06	0.016
Experimental	47.8	3 (1.55, 1.45)	3.3	0.05

Table 14. Comparison of simulation and experimental results of proposed adaptive droop control for varying load and different cable resistances.

Method	V_L (V)	I_L (I_1, I_2) (A)	I_{Error} (%)	$\lvert I_{Cir} \rvert$ (A)
Simulation	47.8	3 (1.54, 1.46)	2.6	0.04
Experimental	47.8	3 (1.6, 1.4)	6.6	0.1

The load sharing error and circulating current results of both the simulation and experimental method show the effectiveness of the proposed adaptive droop control.

6. Conclusions

In this paper, we proposed a simple and robust adaptive droop control based on mathematical calculations, adjusting the droop parameters accordingly. The proposed method computed the droop resistance values instantaneously for any change in source voltage causing a variation in the output voltage of the converter. The proposed algorithm gave a proper load current sharing of the converters. The phenomena of circulating current reduced with the stability of maintaining proper load current sharing between converters as it reduced the difference between the converter currents. With the instantaneous droop resistance calculation, the voltage regulation greatly improved. The effects of varying load and different converter cable resistances were also considered and the effectiveness of the proposed control strategy was analyzed and demonstrated through simulation and experimental studies. The proposed mathematical model was limited to two parallel converters, peak overshoot phenomena were observed at the start, and slight disturbances were present in the load voltage during the variations in the source voltage or load. The future scope is to develop a generalized mathematical model suitable for multiple converters in a DC microgrid, to develop proper tuning of the PI controller to overcome the above-stated effects, and to implement them in real-time applications.

Author Contributions: Conceptualization, P.K.G.R. and S.D.; methodology, P.K.G.R.; software, P.K.G.R.; validation, P.K.G.R., S.D. and V.K.; investigation, P.K.G.R.; writing—original draft preparation, P.K.G.R.; writing—review and editing, S.D.; supervision, S.D. All authors have read and agreed to the published version of the manuscript.

Funding: This research received no external funding.

Institutional Review Board Statement: Not applicable.

Informed Consent Statement: Not applicable.

Data Availability Statement: Not applicable.

Conflicts of Interest: The authors declare no conflict of interest.

References

1. Lexuen, M.; Qobad, S.; Fulwani, D.; Fulwani, F.; Josep, J. Review on control of dc-microgrid. *IEEE Emerg. Selec.* **2017**, *5*, 928–948.
2. Rashad, M.; Raoof, U.; Ashraf, M.; Ahmed, B.A. Proportional load sharing and stability of DC microgrid with distributed architecture using sm controller. *Math. Probl. Eng.* **2018**, *2018*, 1–16. [CrossRef] [PubMed]
3. Patrao, I.; Figueres, E.; Garcerá, G.; González-Medina, R. Microgrid architectures for low voltage distributed generation. *Renew. Sustain. Energy Rev.* **2015**, *43*, 415–424. [CrossRef]
4. Tummuru, N.R.; Mishra, M.K.; Srinivas, S. Multifunctional vsc controlled microgrid using instantaneous symmetrical components theory. *IEEE Trans. Sustain. Energy* **2013**, *5*, 313–322. [CrossRef]
5. Papadimitriou, C.; Zountouridou, E.; Hatziargyriou, N. Review of hierarchical control in DC microgrids. *Electr. Power Syst. Res.* **2015**, *122*, 159–167. [CrossRef]
6. Dragicevic, T.; Lu, X.; Vasquez, J.C.; Guerrero, J.M. DC microgrids—Part I: A review of control strategies and stabilization techniques. *IEEE Trans. Power Electron.* **2015**, *31*, 4876–4891. [CrossRef]
7. Basak, P.; Chowdhury, S.; Dey, S.H.n.; Chowdhury, S. A literature review on integration of distributed energy resources in the perspective of control, protection and stability of microgrid. *Renew. Sustain. Energy Rev.* **2012**, *16*, 5545–5556. [CrossRef]
8. Kakigano, H.; Miura, Y.; Ise, T. Low-voltage bipolar-type dc microgrid for super high quality distribution. *IEEE Trans. Power Electron.* **2010**, *25*, 3066–3075. [CrossRef]

9. Anand, S.; Fernandes, B.G. Optimal voltage level for DC microgrids. In Proceedings of the IECON 2010—36th Annual Conference on IEEE Industrial Electronics Society, Glendale, AZ, USA, 7–10 November 2010; pp. 3034–3039.
10. Planas, E.; Andreu, J.; Gárate, I.; de Alegría, I.M.; Ibarra, E. AC and DC technology in microgrids: A review. *Renew. Sustain. Energy Rev.* **2015**, *43*, 726–749. [CrossRef]
11. Jin, C.; Wang, P.; Xiao, J.; Tang, Y.; Choo, F.H. Implementation of Hierarchical Control in DC Microgrids. *IEEE Trans. Ind. Electron.* **2014**, *61*, 4032–4042. [CrossRef]
12. Baranwal, M.; Askarian, A.; Salapaka, S.; Salapaka, M. A Distributed Architecture for Robust and Optimal Control of DC Microgrids. *IEEE Trans. Ind. Electron.* **2019**, *66*, 3082–3092. [CrossRef]
13. Sahoo, S.K.; Sinha, A.K.; Kishore, N.K. Control Techniques in AC, DC, and Hybrid AC–DC Microgrid: A Review. *IEEE J. Emerg. Sel. Top. Power Electron.* **2018**, *6*, 738–759. [CrossRef]
14. Augustine, S.; Mishra, M.K.; Lakshminarasamma, N. Circulating current minimization and current sharing control of parallel boost converters based on Droop Index. In Proceedings of the 2013 9th IEEE International Symposium on Diagnostics for Electric Machines, Power Electronics and Drives (SDEMPED), Valencia, Spain, 27–30 August 2013; pp. 454–460.
15. Xing, K.; Guo, Y.; Lee, F.; Manners, B. Modeling and dynamic analysis of paralleled DC-DC converter with master/slave current sharing control. In Proceedings of the Applied Power Electronics Conference. APEC' 96, San Jose, CA, USA, 3–7 March 1996; Volume 2, pp. 678–684.
16. Perreault, D.J.; Selders, R.L., Jr.; Kassakian, J.G. Frequency-based current-sharing techniques for paralleled power converters. *IEEE Trans. Power Electron.* **1998**, *13*, 626–634. [CrossRef]
17. Jiang, W.; Fahimi, B. Active current sharing and source management in fuel cell-battery hybrid power system. *IEEE Trans. Ind. Electron.* **2010**, *57*, 752–761. [CrossRef]
18. Luo, S.; Ye, Z.; Lin, R.-L.; Lee, F. A classification and evaluation of paralleling methods for power supply modules. In Proceedings of the 30th Annual IEEE Power Electronics Specialists Conference, Charleston, SC, USA, 1 July 1999; pp. 901–908.
19. Thomas, V.; Kumaravel, S.; Ashok, S. Control of parallel DC-DC converters in a DC microgrid using virtual output impedance method. In Proceedings of the 2016 2nd International Conference on Advances in Electrical Electronics, Information, Communication and Bio-Informatics (AEEICB), Chennai, India, 27–28 February 2016; pp. 587–591.
20. Irving, B.T.; Jovanovic, M.M. Analysis, design, and performance evaluation of droop current-sharing method. In Proceedings of the APEC 2000. Fifteenth Annual IEEE Applied Power Electronics Conference and Exposition (Cat. No.00CH37058), New Orleans, LA, USA, 6–10 February 2000; Volume 1, pp. 235–241.
21. Kim, J.-W.; Choi, H.-S.; Cho, B.H. A novel droop method for converter parallel operation. *IEEE Trans. Power Electron.* **2002**, *17*, 25–32. [CrossRef]
22. Bharath, K.R.; Student, A.D.; Kanakasabapathy, P. A simulation study on modified droop control for improved voltage regulation in DC microgrid. In Proceedings of the 2017 International Conference on Intelligent Computing, Instrumentation and Control Technologies (ICICICT), Kannur, India, 6–7 July 2017; pp. 314–319.
23. Zammit, D.; Staines, C.S.; Apap, M.; Micallef, A. Paralleling of buck converters for DC microgrid operation. In Proceedings of the 2016 International Conference on Control, Decision and Information Technologies (CoDIT), St. Julian's, Malta, 6–8 April 2016; pp. 70–76.
24. Zammit, D.; Staines, C.S.; Apap, M.; Micallef, A. Alternative droop control method using a modified lag compensator for paralleled converters in DC microgrids. In Proceedings of the 2019 6th International Conference on Control, Decision and Information Technologies (CoDIT), Paris, France, 23–26 April 2019; pp. 156–164.
25. Augustine, S.; Mishra, M.K.; Lakshminarasamma, N. Adaptive droop control strategy for load sharing and circulating current minimization in low-voltage standalone DC microgrid. *IEEE Trans. Sustain. Energy* **2015**, *6*, 132–141. [CrossRef]
26. Shehata, E.G.; Thomas, J.; Mostafa, R.M.; Ghalib, M.A. An improved droop control for a low voltage DC microgrid operation. In Proceedings of the 2018 Twentieth International Middle East Power Systems Conference (MEPCON), Cairo, Egypt, 18–20 December 2018; pp. 850–855.
27. Ali, S.; Shengxue, T.; Jianyu, Z.; Ali, A.; Nawaz, A. An implementation of parallel buck converters for common load sharing in DC microgrid. *Information* **2019**, *10*, 91. [CrossRef]
28. Ghanbari, N.; Bhattacharya, S. Adaptive droop control method for suppressing circulating currents in DC microgrids. *IEEE Open Access J. Power Energy* **2020**, *7*, 100–110. [CrossRef]
29. Mohammadi, J.; Ajaei, F.B. Improved mode-adaptive droop control strategy for the DC microgrid. *IEEE Access* **2019**, *7*, 86421–86435. [CrossRef]
30. Zhang, N.; Sun, Q.; Wang, J.; Yang, L. Distributed adaptive dual control via consensus algorithm in the energy internet. *IEEE Trans. Ind. Inform.* **2021**, *17*, 4848–4860. [CrossRef]
31. Hafiz, F.; Awal, M.A.; De Queiroz, A.R.; Husain, I. Real-time stochastic optimization of energy storage management using deep learning-based forecasts for residential PV applications. *IEEE Trans. Ind. Appl.* **2020**, *56*, 2216–2226. [CrossRef]
32. Li, Y.; Gao, D.W.; Gao, W.; Zhang, H.; Zhou, J. A distributed double-newton descent algorithm for cooperative energy management of multiple energy bodies in energy internet. *IEEE Trans. Ind. Inform.* **2021**, *17*, 5993–6003. [CrossRef]